Preparation and Characterization of Cubic and Hexagonal Polytypes of ZnSe:Cu2+ One-Dimensional Nanostructures

ARTICLE *in* THE JOURNAL OF PHYSICAL CHEMISTRY C · MARCH 2008

Impact Factor: 4.77 · DOI: 10.1021/jp710764m

7 AUTHORS, INCLUDING:

Baojuan xi
National University of Singapore
37 PUBLICATIONS **1,289** CITATIONS

SEE PROFILE

Chengming Wang
University of Science and Technology of China
96 PUBLICATIONS **705** CITATIONS

SEE PROFILE

Preparation and Characterization of Cubic and Hexagonal Polytypes of ZnSe:Cu^{2+} One-Dimensional Nanostructures

Baojuan Xi,[†] Dechen Xu,[†] Shenglin Xiong,[†,‡,§] Chengming Wang,[§] Xiaoming Feng,[§] Hongyang Zhou,[†] and Yitai Qian*[,†,‡,§]

Department of Chemistry, Department of Materials Science and Engineering, and Hefei National Laboratory for Physical Sciences at Microscale, University of Science and Technology of China, Hefei, Anhui, 230026 China

Received: November 10, 2007; In Final Form: January 17, 2008

Cu-doped ZnSe single-crystal one-dimensional (1-D) nanostructures were fabricated via thermal treatment of the as-synthesized corresponding precursor, which was prepared through a ternary solution-based method. The evident phase transformation suggests that doping with Cu^{2+} favors the formation of the cubic phase ZnSe. The as-prepared products were characterized using diverse techniques (X-ray powder diffraction, high-resolution transmission electron microscopy, and selected area electron diffraction), which demonstrate that both the sphalerite cubic phase and the wurtzite hexagonal phase coexist in nanowires obtained from ZnSe doped with different amounts of Cu^{2+}.

Introduction

One-dimensional (1-D) nanoscale semiconductor building blocks, such as nanowires and nanobelts, have attracted considerable attention in recent years because of their potential applications as optoelectronic materials in various fields. In particular, as a valuable semiconductor with a room-temperature bulk band gap of 2.70 eV (460 nm), ZnSe-based nanostructures have been the focus of intense scientific research due to their potential applications in UV light-emitting devices, light-emitting diodes (LEDs), blue-light-emitting lasers, and photodetectors.[1] Furthermore, ZnSe holds a much larger exciton binding energy (21 meV)[2] in comparison to that of GaAs (4.2 meV),[3] which makes it an excellent candidate for exploring the intrinsic recombination process in efficient room-temperature exciton devices. Therefore, the synthesis and optical properties of ZnSe nanocrystals have been investigated widely.

To date, many synthetic methods have been developed to prepare ZnSe nanocrystals with different morphologies such as nanowires (nanobelts), microtubes, and microspheres.[4] These pioneering achievements have prompted researchers to go beyond pure nanocrystals and to investigate nanostructures intentionally doped with impurities. During the past several years, much effort has focused on II−VI semiconductor nanocrystals that were doped with Mn, Cr, or Ag. For instance, ZnSe colloidal nanocrystals doped with paramagnetic Mn^{2+} impurities have been reported to show a high fluorescence.[5] Photoluminescence of Ag-doped ZnSe nanowires synthesized by MCVD was investigated in detail within the temperature range of 10−300 K.[6]

Recently, our group has introduced a solvothermal approach in a homogeneous mixed solution to various ZnS hierarchical structures,[7a] complex CdS in various 3- and 1-D structures,[7b] and wurtzite ZnSe ultrathin nanobelts.[4j] Herein, we fabricated single-crystalline-doped ZnSe 1-D nanostructures via the thermal treatment of the as-synthesized precursors that were prepared through a ternary solution-based method. In comparison to the loss process of ethylenediamine in the preparation of 1-D undoped ZnSe nanowire bundles,[4f] the introduction of transition metal ions such as Cu^{2+} and others into ZnSe 1-D nanostructures may change the thermodynamic and kinetic factors of the process, which results in the coexistence of both cubic and hexagonal phases in the nanowires.

Experimental Procedures

Materials. Zinc sulfate ($ZnSO_4 \cdot 7H_2O$), copper sulfate ($CuSO_4 \cdot 5H_2O$), ethylenediamine (en), deionized water, selenium power, and hydrazine hydrate ($N_2H_4 \cdot H_2O$) were of analytical grade (purchased from Shanghai Chemical Industrial Co.) and were used without further purification.

Synthesis. In a typical synthesis, anhydrous ethylenediamine (25 mL) was added to an aqueous solution, $ZnSO_4 \cdot 7H_2O$ (12 mL, 2mmol). Different quantities of the reactants, $CuSO_4 \cdot 5H_2O$, were added to the solution and magnetically stirred for 10 min, the solution was transferred to a 50 mL stainless Teflon lined autoclave, and then selenium (0.158 g, 2 mmol) and hydrazine hydrate (5 mL, $N_2H_4 \cdot H_2O$) were put directly into the autoclave. The autoclave was sealed and maintained at 180 °C for 20 h and finally allowed to cool to room temperature. The final product was collected by filtration, then repeatedly washed with distilled water and absolute alcohol, and at last vacuum-dried. To remove ethylenediamine and to obtain ZnSe:Cu^{2+} nanowires, the as-prepared precursor was calcined in a tube furnace at 500−600 °C under a pure argon atmosphere for 4−6 h.

Characterization. The XRD analysis was performed using a Japanese Rigaku D/max-γA rotating anode X-ray diffractometer equipped with monochromatic high-intensity Cu Kα radiation ($\lambda = 1.54178$). The X-ray photoelectron spectra (XPS) were collected on an ESCALab MKII X-ray photoelectron spectrometer, using nonmonochromatized Mg Kα X-rays as the excitation source. Field emission scanning electron microscopy (FESEM) images were taken on a JEOL JSM-6300F SEM.

* To whom correspondence should be addressed. E-mail: ytqian@ustc.edu.cn; tel.: 86-551-3607234; fax: 86-551-3607402.
[†] Department of Chemistry.
[‡] Department of Materials Science and Engineering.
[§] Hefei National Laboratory for Physical Sciences at Microscale.

10.1021/jp710764m CCC: $40.75
Published on Web 03/19/2008

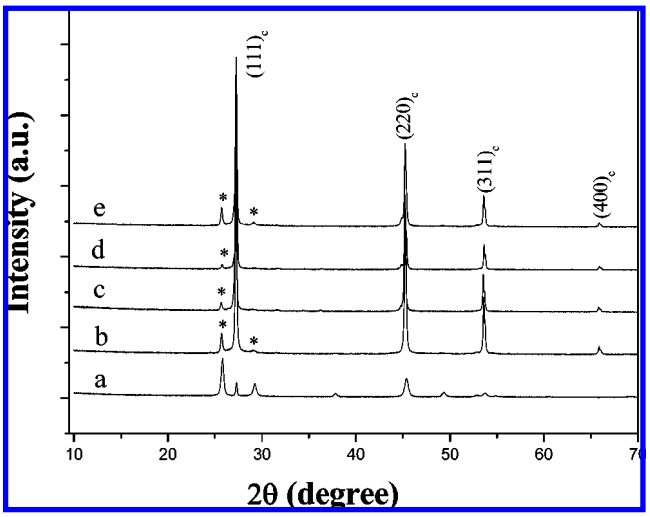

Figure 1. X-ray diffraction of the as-obtained ZnSe:Cu^{2+} nanowires obtained by thermal treatment of the corresponding precursor at 600 °C in an inert atmosphere from different Zn/Cu sources revealing the existence of cubic and hexagonal phase ZnSe (asterisk show XRD peaks of hexagonal ZnSe). (a) Zn/Cu = ∞, (b) Zn/Cu = 20:1, (c) Zn/Cu = 20:1.5, (d) Zn/Cu = 20:2.5, and (e) Zn/Cu = 20:3.

Transmission electron microscopy (TEM) and electron diffraction (ED) patterns were taken with a Hitachi Model H-800 instrument using an accelerating voltage of 200 kV with a tungsten filament. High-resolution TEM (HRTEM) images and SAED patterns were obtained on a JEOL-2010 transmission electron microscope at an acceleration voltage of 200 kV. Thermogravimetric analysis (TGA) of the precursor was recorded on a TGA-2050 (TA Corp.) thermogravimeter. EDX spectra were measured using the HRTEM instrument.

Results and Discussion

The phase and chemical composition of the as-synthesized Cu-doped ZnSe 1-D nanostructures were examined by XRD shown in Figure 1, which indicates the phase transition of the products. When the products were prepared in the absence of $CuSO_4$, all the reflections of as-synthesized ZnSe could be readily indexed to the hexagonal phase of ZnSe with lattice constants a = 3.997 Å and c = 6.547 Å (JCPDS card no. 80−0008). It is worth pointing out that both zinc blende (cubic) and wurtzite (hexagonal) phases coexist in the nanowires with increasing the mole ratio of Zn/Cu from 20:1 to 20:3, which is consistent with the following HRTEM results. Sharp and strong peaks also demonstrated that the as-obtained products were well-crystallized under the current synthetic conditions. However, when the thermal treatment temperature of these precursors was increased to 700−800 °C, the reflections of Cu-doped ZnSe could be readily indexed to the pure cubic phase ZnSe with a calculated lattice constant a = 5.656 Å, which agrees with the reported data (a = 5.618 Å, JCPDS card no. 80−-0021, whereas the undoped ZnSe products still remained in the hexagonal phase (see Figure S1 in the Supporting Information). No other impurity peaks were detected. Therefore, the obvious phase transformation implies that Cu doping is in favor of the formation of the new phase of sphalerite structure ZnSe in the present experimental conditions.

The morphology of the corresponding precursors was investigated by TEM (see Figure S2 in the Supporting Information), revealing that most of the as-obtained precursors were both belt- and wire-like nanostructures. The TGA curve of the Cu-doped ZnSe precursor is shown in Figure 2. There are two weight loss steps as the temperature ranges from 40− to 193 and 193− to 557 °C. The first weight loss mainly results from the evaporation of H_2O, whereas the second loss could be attributed to the decomposition of the precursor. The weight loss during the second step was about 18.9%. On the basis of the experimental results, assuming the chemical formula of the precursor is ZnSe:Cu^{2+}·x(ethylenediamine), calculations based on the TGA results gave a value of x equal to 0.5 for the precursor within experimental error, which is different from the value of the undoped ZnSe precursor.[4f,8] However, this is consistent with the value that previously was reported.[9] It might be ascribed to the doped metal ions in the precursor, considering that many kinds of diamine-intercalated materials, including CdS·0.5en and ZnTe-(N_2H_4), have been investigated to have layered structures.[10,11] The present en-intercalated ZnSe:Cu^{2+} might have a similar layered structure. Direct evidence for this hypothesis requires structural determination; further work is underway.

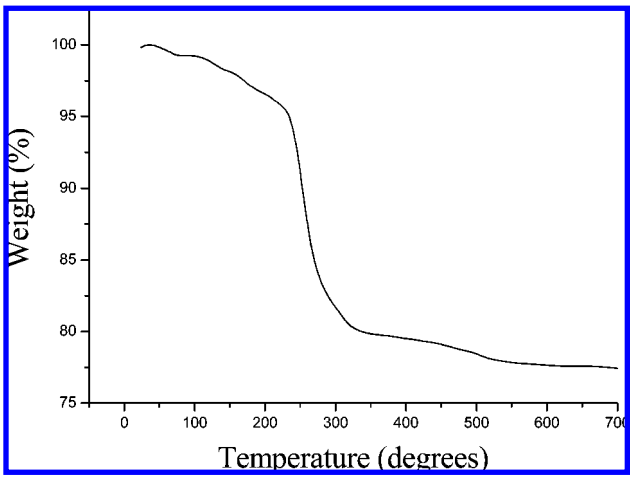

Figure 2. TGA curve of the Cu-doped ZnSe 1-D nanostructure obtained from the mole ratio of Zn/Cu = 20:3.

Evidence for the composition of the doped sample (ZnSe:Cu^{2+}) was observed from the XPS images of the products (see Figure 3). The strong peaks at 1022.02 and 54.06 eV corresponding to Zn 2p and Se 3d binding energies, respectively, were observed, while the binding energy at 931.42 eV for Cu 2p demonstrates the existence of Cu^{2+} ions in the nanowires. Table 1 reveals the average mole fraction of the element Cu in the sample. As compared to the starting compositions, the mole fraction of Cu becomes small, which could result from the special reaction and specific starting material in our current synthetic system. In addition, some carbon and oxygen contamination mainly from the surface of the nanowires also can be detected. The concentrations of dopant ions present in the starting materials and final decomposed products were further estimated using elemental analysis with energy-dispersive X-ray spectroscopy (EDX), which was performed on different regions of several random nanowires in the sample (the signals of Mo are from the molybdenum grid), consistent with the results of XPS (Table 2).

The elemental analysis with EDS shown in Figure 4e demonstrates that the mole ratio of Zn and S is 1.157:1 (the signals of Cu are from the copper grid), which is close to that of the standard stoichiometric composition, consistent with the results of XPS (see Supporting Information Figure S2a).

A subsequent FESEM study revealed that the morphology of the as-synthesized products gradually changed by relying on the dopant ratio. Figure 4b indicates that the product is composed of a large amount of bundles of nanowires with diameters ranging from 40 to 60 nm and lengths of up to tens of

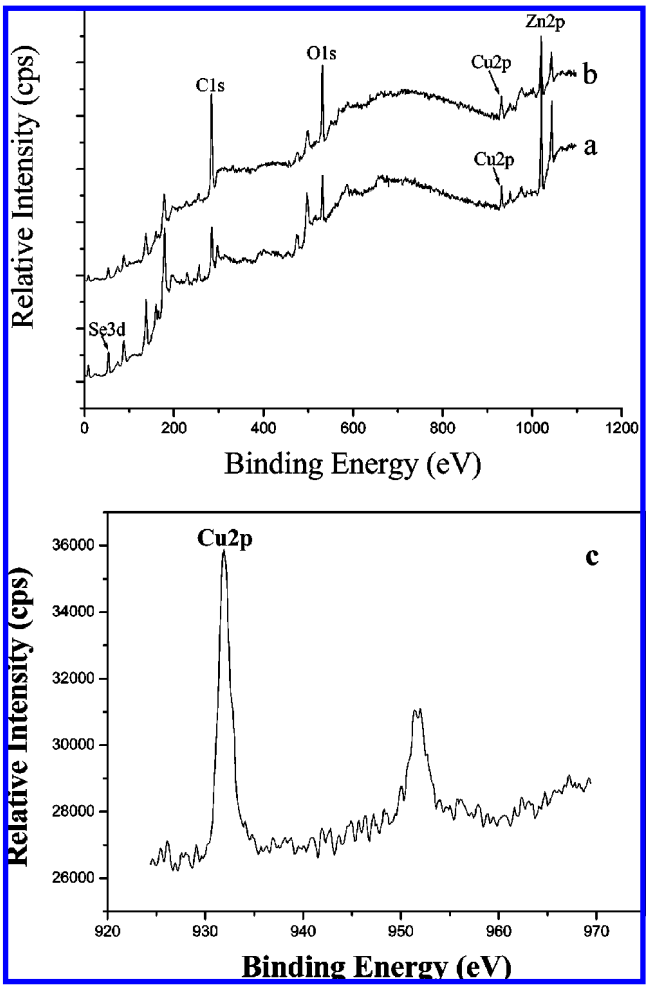

Figure 3. XPS spectra of Cu-doped ZnSe nanowires obtained from different Zn/Cu sources. (a) Zn/Cu = 20:1.5 and (b) Zn/Cu = 20:3. Some carbon and oxygen contamination mainly from the surface of the nanowires also can be observed. (c) Enlarged surveys for Cu 2p obtained from the mole ratio of Zn/Cu = 20:3.

TABLE 1: Mole Fraction (Mol %) of Cu in Starting Materials and in Products

starting material (Cu/Zn)	products/Cu (mol %)
1.0:20	4.34
2.0:20	6.58
2.5:20	10.47

TABLE 2: Mole Fraction (Mol %) of Cu in Starting Materials and in Products, Measured by Energy-Dispersive X-ray Spectroscopy (EDX)

starting material (Cu/Zn)	products/Cu (mol %)
1.0:20	4.12
2.0:20	8.96
2.5:20	11.08

micrometers when Cu/Zn = 1:20 was used as the reaction material. During the preparation process, we observed that the morphology of the as-obtained nanostructures was sensitive to the addition to the quantity of $CuSO_4$ in the reaction system, as compared to the undoped sample (see Figure 4a). When Zn/Cu = 20:1.5 was adopted as the source, wire-like nanostructures were obtained (Figure 4c). With the increase of the amount of $CuSO_4$, the shape of the products gradually changed from nanowire bundles to near-helical and bone-like nanowires (as shown by arrows in Figure 4). At the same time, the diameter of the nanowires obviously increased. Similar wire-like 1-D nanostructures could be synthesized when Zn/Cu = 20:2.5 was used as the starting source (see Figure 4d). It is worth noting that the surface of these nanowires gradually became rougher and at the same time contained a fraction of the broken fragment with an increase of the dopant. More detailed TEM observations showed that there were various forms of wire-like structures that included near-helical, bone-like, tapered, and branch-like nanostructures, as indicated in Figure 5. On the basis of the previous results, we believe that the morphology of the products could be well-controlled by varying the quantity of the dopant.

To better understand the structural characteristics of the as-synthesized Cu-doped ZnSe 1-D nanostructures, we studied the microstructure of the Cu-doped ZnSe nanowires using HRTEM. It is worth noting that, for the more than 100 nanowires examined, HRTEM images have given us further insight into the structure and actually demonstrated that both sphalerite cubic and wurtzite hexagonal phases coexist in nanowires obtained from different Zn/Cu sources, which is the growth direction of these nanowires. Figure 6a indicates the typical low-magnification TEM images of such ZnSe:Cu nanowires (Zn/Cu = 20:1 as the source). The corresponding ED pattern and HRTEM image are shown in Figure 6b,c, respectively. The ED pattern can be indexed to two sets of diffraction reflections of the [100] zone axis of the single crystal with the wurtzite structure (hcp, hexagonal close-packed) and that of the [110] zone axis with the sphalerite structure (fcc, face-centered cubic) as shown. The corresponding HRTEM image (in Figure 6c) clearly reveals that two phases (cubic and hexagonal) coexist in this individual nanowire observed region (with a measured hexagonal phase interplanar spacing of about 0.65 nm and cubic phase spacing of crystallographic planes of about 0.37 nm), both of which are consistent with the interplanar spacing of the (001) planes of wurtzite ZnSe and the (111) planes of sphalerite ZnSe. These results are in agreement with the previous XRD conclusions. The lattice planes, exhibiting bright spots parallel to the length axis of the nanowires, are both close-packed (002) plane of the hcp structure and (111) plane of the fcc structure, respectively. The [120] direction of the hcp structure zone is parallel to the [112] direction of the fcc zone, which can be assigned to the growth direction of the nanowires.

Figure 7a−c are typical low-magnification TEM images of ZnSe nanowires with diameters of about 50−200 nm when Zn/Cu = 20:1.5, 20:2, and 20:2.5 were used as the reaction source, respectively. The corresponding HRTEM results shown in Figure 8d−f reveal that both cubic and hexagonal phases coexist in these nanowires obtained from different Zn/Cu sources, which is the growth direction of these nanowires. Lattice fringe details show that the interface between regions B and C, as well as between regions D and E, is twins (T) in the sphalerite structure zone (in Figure 7d), whereas the stacking faults (SF) exist in the wurtzite structure regions as shown (see Figures 6c and 7f). These two phases' coexistence structure properties of as-made Cu-doped ZnSe nanowires almost could not be found in the undoped ZnSe 1-D nanostructure. This could be deduced because these two types of structures coexist by changing the stacking sequence of the close-packed planes of the ZnSe crystal, which could be attributed to the doped Cu ions.

As we know, the sphalerite and wurtzite ZnSe crystals can both can act as a stack of $ZnSe_4$ tetrahedra through sharing their common corners, in addition to the stacking modes of the two-layer tetrahedron. Similar to that of ZnS,[12] the growth orientation of the ZnSe crystal was determined by the relative stacking rate of the tetrahedron and the bonding force of the various atoms. With regard to the ZnSe crystal, the (001) planes and the (111) planes are both close-packed planes of the hcp structure and

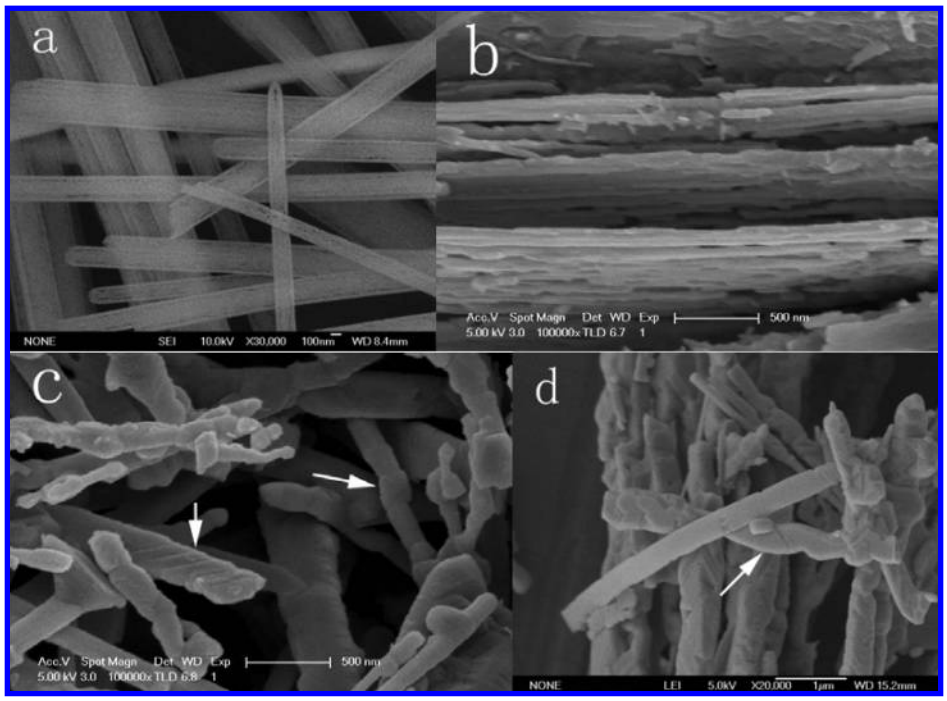

Figure 4. FESEM images of the ZnSe:Cu^{2+} 1-D nanostructures obtained from different Zn/Cu sources. (a) Undoped ZnSe, (b) Zn/Cu = 20:1, (c) Zn/Cu = 20:1.5, and (d) Zn/Cu = 20:2.5.

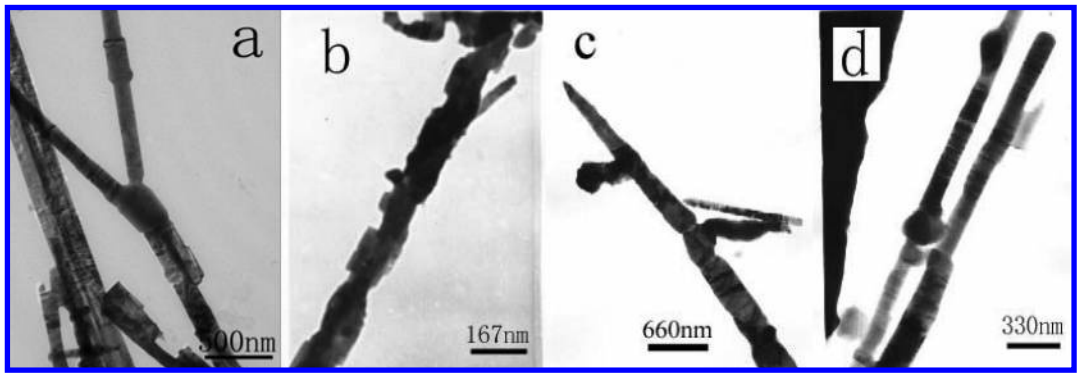

Figure 5. TEM image of the ZnSe/Cu^{2+} 1-D nanostructure obtained from different Zn/Cu sources. (a) Zn/Cu = 20:1.5, (b) Zn/Cu = 20:2.0, and (c and d) Zn/Cu = 20:2.5.

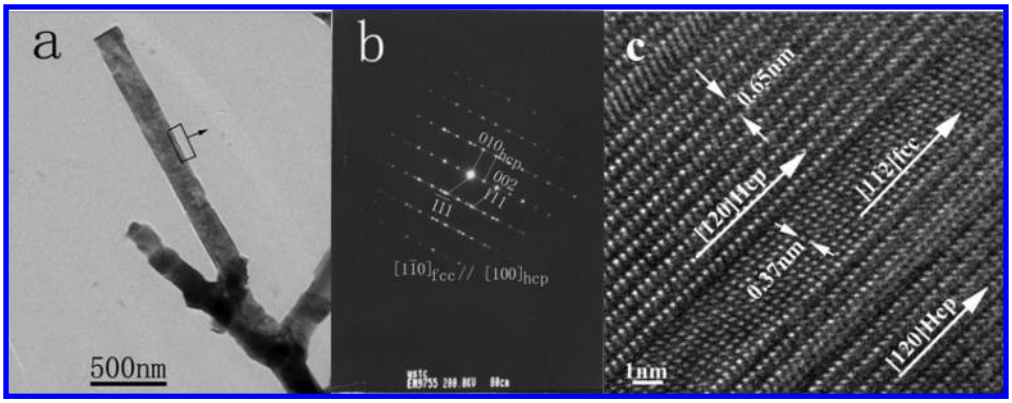

Figure 6. (a) TEM image of a branch-like ZnSe nanowire, (b) corresponding SAED pattern, and (c) corresponding HRTEM image show that the wurtzite structure and sphalerite structure are formed by changing the stacking sequence of close-packed planes of the ZnSe crystal.

the fcc structure. As a result, they have a preferential stacking rate, which favors the growth along the [001] and [111] axes, respectively. Recently, Lieber and Duan[13] reported that many wurtzite semiconductors exist prior to the growth along the [001] direction, while sphalerite can grow along the [111] orientation, which is in good agreement with our as-obtained results.

Further advancement of this approach of the 1-D nanostructure with different shape synthesis requires a clear understanding

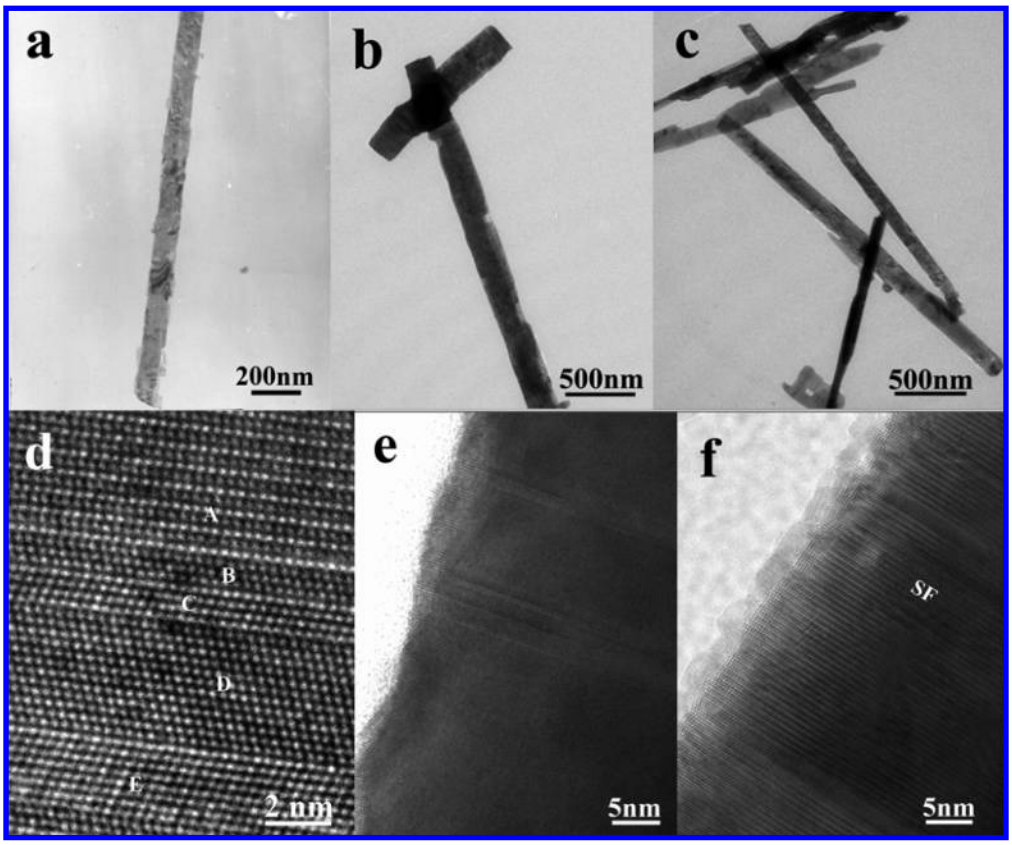

Figure 7. (a−c) Low-magnification TEM images of ZnSe nanowires obtained when Zn/Cu = 20:1.5, 20:2, and 20:2.5 acted as the reaction source, respectively. (d−f) Corresponding HRTEM images of the ZnSe nanowires shown in panels a−c, showing that both cubic and hexagonal phases coexist in these nanowires.

of the nucleation and growth mechanism, including both the formation process of the precursor and the thermal treatment process of the precursor. The chemical reaction involved in the formation of the precursor can be formulated as follows:

$$Zn^{2+} + Cu^{2+} + en \xrightarrow{\text{solvothermal}} [Zn^{2+}{:}Cu^{2+}](en)_{0.5} \quad (1)$$

$$Se^{2-} \xrightarrow{N_2H_4\cdot H_2O} H_2O\cdot Se^{2-} \quad (2)$$

$$[Zn^{2+}{:}Cu^{2+}](en)_{0.5} + Se^{2-} \rightarrow [ZnSe{:}Cu^{2+}](en)_{0.5} \quad (3)$$

In calcination treatment, the precursor decomposed into ZnSe and ethylenediamine, and the chemical reaction could be formatted as the following equation:

$$[ZnSe{:}Cu^{2+}](en)_{0.5} \xrightarrow{600\ ^\circ C} ZnSe{:}Cu^{2+} \quad (4)$$

It should be pointed out that the belt-like $[ZnSe{:}Cu^{2+}]$-$(ethylenediamine)_{0.5}$ could be prepared only in a ternary solution with a proper volume ratio of $V_{en}/V_{H_2O}/V_{N_2H_4\cdot H_2O}$. On the basis of our results, in the absence of any of the three solvents under the same experimental conditions, no ribbon-like ZnSe precursors were prepared. Obviously, the synergistic effects of the ternary solution could play a very key role in the formation process of the belt-like precursor. The precursor could be further converted to 1-D ZnSe nanostructures, owing to the loss of ethylenediamine. As we know, the loss of ethylenediamine from the undoped precursor to form individual ZnSe nanowires under a ternary solution is difficult, possibly due to unfavorable thermodynamic and kinetic factors, which could arise from the strong coordination effect of ethylendiamine to zinc (log β of $[Zn(en)_3]^{2+}$ is 14.11). However, in the present experimental conditions, a large number of individual wire-like nanostructures with various shapes were formed, which might lead to changes in the thermodynamic and kinetic factors during the loss process of ethylenediamine, possibly resulting from the addition of the doped cations. At the same time, the phase transformation of wurtzite (hexagonal ZnSe) to zinc-blende (cubic ZnSe) could be explained according to a periodic slip mechanism[14−16] involving the expansion of stacking faults around an axial screw dislocation, possibly due to the dopant entrance into ZnSe nanowires. Herein, our results could further validate the mechanism. On the other hand, the doped metal ions could act as a catalyst to catalyze the growth of the wire-like 1-D nanostructure and, in the meantime, favor the phase transformation process due to transition metals and their compounds often having some catalytic effect. Of course, it should be pointed out that the present ternary solution reaction system and the calcinations of the process are quite complicated and that the detailed the growth process needs to be resolved further.

Conclusion

In conclusion, ZnSe:Cu^{2+} single-crystal 1-D nanostructures were fabricated via the thermal treatment of the as-synthesized corresponding precursor, which was prepared through a ternary solution. HRTEM images and ED demonstrated that both sphalerite cubic and wurtzite hexagonal phases coexist in nanowires obtained from different Zn/Cu sources, which could be formed by changing the stacking sequence of the close-packed planes of the ZnSe crystal due to the addition of doping. Meanwhile, we believe that the present convenient method could be extended to prepare other doped semiconductor 1-D nano-

structures by an appropriate choice of reaction system and experimental conditions. Further work is still in progress.

Acknowledgment. Financial support of this work, by the China Postdoctoral Science Foundation (20070420124), the National Natural Science Foundation of China (20431020), and the 973 Project of China (2005CB623601), is gratefully acknowledged.

Supporting Information Available: XRD spectrum for as-synthesized Cu-doped and undoped ZnSe obtained by thermal treatment of precursor at 800 °C in inert atmosphere and TEM images of the doped ZnSe precursors obtained from different ZnSe:Cu sources. This material is available free of charge via the Internet at http://pubs.acs.org.

References and Notes

(1) (a) Haase, M. A.; Qiu, J.; Depuydt, J. M.; Cheng, H. *Appl. Phys. Lett.* **1991**, *59*, 1272. (b) Passler, R.; Griebl, E.; Ripel, H.; Lautner, G. et al. *J. Appl. Phys.* **1999**, *86*, 4403. (c) Wang, J.; Hutchings, D. C.; Miller, A. et al. *J. Appl. Phys.* **1993**, *73*, 4746.

(2) Zhu, Z. M.; Liu, N. Z.; Li, G. H.; Han, H. X.; Wang, Z. P.; Wang, S. Z.; He, L.; Ji, R. B.; Wu, Y. *J. Infrared Millimeter Waves* **1999**, *18*, 13.

(3) Wang, S. Z.; Yoon, S. F.; He, L.; Shen, X. C. *J. Appl. Phys.* **2001**, *90*, 2314.

(4) (a) Jiang, Y.; Meng, X. M.; Yiu, W. C.; Liu, J.; Ding, J. X.; Lee, C. S.; Lee, S. T. *J. Phys. Chem. B* **2004**, *108*, 2787. (b) Li, Q.; Gong, X. G.; Wang, C. R.; Wang, J.; Ip, K.; Hark, S. K. *Adv. Mater.* **2004**, *16*, 1436. (c) Zhang, X. T.; Liu, Z.; Ip, K. M.; Leung, Y. P.; Li, Q.; Hark, S. K. *J. Appl. Phys.* **2004**, *95*, 5752. (d) Zhu, Y. C.; Bando, Y. *Chem. Phys. Lett.* **2003**, *377*, 367. (e) Solanki, R.; Huo, J.; Freeouf, J. L. *Appl. Phys. Lett.* **2002**, *81*, 3864. (f) Xiong, S. L.; Shen, J. M.; Xie, Q.; Gao, Y. Q.; Tang, Q.; Qian, Y. T. *Adv. Funct. Mater.* **2005**, *15*, 1787. (g) Hu, J. Q.; Baobo, Y.; Zhan, J. H.; Liu, Z. W.; Golberg, D.; Ringer, S. P. *Adv. Mater.* **2005**, *17*, 975. (h) Peng, Q.; Dong, Y. J.; Li, Y. D. *Angew. Chem., Int. Ed.* **2003**, *42*, 3027. (i) Yao, W. T.; Yu, S. H.; Jiang, J.; Zhang, L. *Chem.—Eur. J.* **2006**, *12*, 2066. (j) Xiong, S. L.; Xi, B. J.; Wang, C. M.; Xi, G. C.; Liu, X. Y.; Qian, Y. T. *Chem.—Eur. J.* **2007**, *13*, 7926.

(5) Norris, D. J.; Yao, N.; Charnock, F. T.; Kennedy, T. A. *Nano Lett.* **2001**, *1*, 3.

(6) Zhang, X. T.; Ip, K. M.; Li, Q.; Hark, S. K. *Appl. Phys. Lett.* **2005**, *86*, 203114.

(7) (a) Xiong, S. L.; Xi, B. J.; Wang, C. M.; Xu, D. C.; Feng, X. M.; Zhu, Z. C.; Qian, Y. T. *Adv. Funct. Mater.* **2007**, *17*, 2728. (b) Xiong, S. L.; Xi, B. J.; Wang, C. M.; Zou, G. F.; Fei, L. F.; Wang, W. Z.; Qian, Y. T. *Chem.—Eur. J.* **2007**, *13*, 3076.

(8) Zhan, J. H.; Yang, X. G.; Zhang, W. X.; Wang, D. W.; Xie, Y.; Qian, Y. T. *J. Mater. Res.* **2000**, *15*, 629.

(9) (a) Deng, Z. X.; Wang, C. H.; Sun, X. M.; Li, Y. D. *Inorg. Chem.* **2002**, *41*, 869. (b) Huang, X. Y.; Li, J.; Fu, H. X. *J. Am. Chem. Soc.* **2000**, *122*, 8789.

(10) Deng, Z. X.; Li, L. B.; Li, Y. D. *Inorg. Chem.* **2003**, *42*, 2331.

(11) Huang, X. Y.; Li, J.; Zhang, Y.; Mascarenhas, A. *J. Am. Chem. Soc.* **2003**, *125*, 7049.

(12) (a) Zhu, Y. C.; Bando, Y.; Xue, D. F. *Appl. Phys. Lett.* **2003**, *82*, 1769. (b) Xue, D.; Zhang, S. *Chem. Phys. Lett.* **1998**, *287*, 503.

(13) Duan, X.; Lieber, C. M. *Adv. Mater.* **2000**, *12*, 298.

(14) Daniels, B. K. *Philos. Mag.* **1966**, *14*, 487.

(15) Mardix, S.; Steinberger, I. T. *Isr. J. Chem.* **1966**, *3*, 243.

(16) Sebastian, M. T.; Krishna, P. *Pramana* **1984**, *23*, 395.